# Absorption enhancement and total absorption in a graphene-waveguide hybrid structure

Cite as: AIP Advances **7**, 025101 (2017); https://doi.org/10.1063/1.4975706
Submitted: 11 November 2016 • Accepted: 23 January 2017 • Published Online: 01 February 2017

**Jun Guo, Leiming Wu, Xiaoyu Dai, et al.**

# Absorption enhancement and total absorption in a graphene-waveguide hybrid structure

Jun Guo, Leiming Wu, Xiaoyu Dai,[a] Yuanjiang Xiang, and Dianyuan Fan
*SZU-NUS Collaborative Innovation Center for Optoelectronic Science and Technology, Key Laboratory of Optoelectronic Devices and Systems of Ministry of Education and Guangdong Province, College of Optoelectronic Engineering, Shenzhen University, Shenzhen 518060, China*

(Received 11 November 2016; accepted 23 January 2017; published online 1 February 2017)

We propose a graphene/planar waveguide hybrid structure, and demonstrate total absorption in the visible wavelength range by means of attenuated total reflectance. The excitation of planar waveguide mode, which has strong near field enhancement and increased light interaction length with graphene, plays a vital role in total absorption. We analyze the origin and physical insight of total absorption theoretically by using an approximated reflectance, and show how to design such hybrid structure numerically. Utilizing the tunability of doped graphene, we discuss the possible application in optical modulators. We also achieve broadband absorption enhancement in near-IR range by cascading multiple graphene-waveguide hybrid structures. We believe our results will be useful not only for potential applications in optical devices, but also for studying other two-dimension materials.  [http://dx.doi.org/10.1063/1.4975706]

## I. INTRODUCTION

Graphene, first experimentally discovered in 2004,[1] is a monolayer of carbon atoms in two dimensional honeycomb lattice. Over the past decade, graphene has been studied intensively due to its extraordinary electronic and optical properties.[2–5] Due to its unique band structure, undoped graphene has a broadband absorption of about 2.3% within visible to infrared wavelength, though the atomic thin layer is only about 0.34nm thick. While after electrically doped, interband absorption will be suppressed for photon energy below $2E_F$, where $E_F$ is the electrically tunable Femi energy. Thus graphene has been applied to realize various optical devices, including optical modulators,[6] photodetectors,[7,8] polarizers[9] and so on.

To realize high performance optical devices above, higher absorption, which means stronger light-matter interaction, is always desired. However absorption of suspended monolayer graphene is too weak due to short interaction length with incident light. So a lot of efforts have been done to enhance absorption of monolayer graphene in the past years. In the mid-IR to THz wavelengthes, doped graphene with negative effective permittivity acts like ultrathin metals, and surface plasmonic polaritons (SPPs) can be excited due to coupling of incident light and electrons in graphene.[10] The excitation of SPPs will cause strong field enhancement near graphene, and strong absorption of graphene can be realized. This method has been widely studied to realize absorption enhancement or even total absorption for graphene strips,[11,12] nano disks[13,14] and metamaterials.[15] However in the visible to near-IR spectrum, wave vector mismatch between graphene SPPs and vacuum light is very large and difficult to compensate, and graphene SPPs can not be excited, very high doping levels or small sized nanostructures are always required[16] which are difficult to realize. Thus extra resonant structures are usually utilized together with monolayer graphene in this spectrum, including Fabry-Perot cavity,[17,18] photonic crystals,[19,20] SPPs of metals[21,22] and critical coupling.[23–25]

[a]Electronic mail: xiaoyudai@126.com

 

While enhanced or total absorption of monolayer graphene has been studied in several works, new structures which can be easily fabricated, robust and have high absorption in a wide spectrum, are always pursued and still need further investigation. In principle, to enhance absorption of graphene, on the one hand we can eliminate the transmittance of incident light, which is the principle of critical coupling. On the other hand, we should enhance light intensity near graphene or equivalently extend interaction length between light and graphene. In our work, we combine all above points together. We use an attenuated total reflectance(ATR) configuration to eliminate transmittance of light, a planar waveguide (PWG) is placed under the prism, and two monolayer graphene are attached on both sides of PWG core. If incident light is at resonant angle, PWG mode will be excited, both strong light intensity enhancement and interaction length extension can be expected for the graphene-PWG hybrid structure. Thus we can get enhanced or even total absorption for the hybrid structure. The proposed structure may have potential application in fabrication of various optical devices especially optical modulators. We also notice that there were works using ATR to enhance graphene absorption,[23,26,27] however extra resonant structures were not included there, total absorption were not achieved.

## II. THEORETICAL MODELS AND METHODS

The structures studied in this work are shown in Fig. 1, where Fig. 1(a) includes one PWG and Fig. 1(b) includes multiple PWGs. The former will be discussed in detail both theoretically and numerically, and the latter will be studied at last to get broadband absorption enhancement. In Fig. 1(a), the proposed structure consists of a single coupling prism with refractive index $n_0$, under which is a graphene-PWG hybrid structure. The first layer with thickness $t_1$ and refractive index $n_1$, and the substrate with refractive index $n_3$ act as cladding layers of PWG. The second layer with thickness $t_2$ and refractive index $n_2$, acts as the core layer of PWG. Two monolayer graphene marked by thick red lines are attached on both sides of core layer. A TE or TM polarized laser beam is incident onto the graphene-PWG hybrid structure from the prism side with incident angle $\theta$. To excite PWG mode in this structure, condition $(n_0, n_2, ) > (n_1, n_3)$ must be satisfied. Thus the PWG core layer and prism is chosen to be boron nitride (BN) ($n_2$=2.1), and the PWG cladding layers are chosen to be silica ($n_1 = n_3 = 1.457$). Here we use BN for not only its high refractive index, but also its compatibility with high quality graphene.[28] Under condition of $n_0 > n_3$, ATR occurs if incident angle is larger than critical angle, and transmission of light will be eliminated, further if the incident angle is at resonant angle of PWG, the PWG mode can be excited.

The reflectance $R$ of the structure is given by:

$$\begin{cases} r_{123} = \frac{r_{12}+[1\pm(r_{12}+r_{21})]r_{23}\exp(2ik_{z2}t_2)}{1-r_{21}r_{23}\exp(2ik_{z2}t_2)} = \frac{\beta}{\alpha} \\ R = |r_{0123}|^2 = \left|\frac{r_{01}+r_{123}\exp(2ik_{z1}t_1)}{1+r_{01}r_{123}\exp(2ik_{z1}t_1)}\right|^2 \end{cases} \tag{1}$$

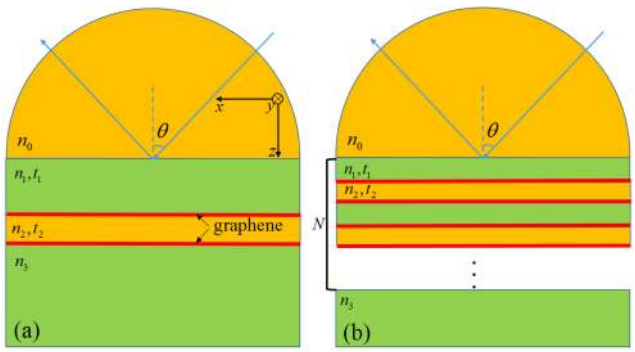


FIG. 1. Schematic of the proposed hybrid structures. (a) Single PWG. (b) $N$ PWGs with 2 period shown.

with

$$\begin{cases} \text{TE}: r_{ij} = \frac{k_{zi} - k_{zj} - \sigma\omega\mu_0}{k_{zi} + k_{zj} + \sigma\omega\mu_0} \\ \text{TM}: r_{ij} = \frac{k_{zi}/\varepsilon_i - k_{zj}/\varepsilon_j + (\sigma/\omega\varepsilon_0)(k_{zi}k_{zj}/\varepsilon_i\varepsilon_j)}{k_{zi}/\varepsilon_i + k_{zj}/\varepsilon_j + (\sigma/\omega\varepsilon_0)(k_{zi}k_{zj}/\varepsilon_i\varepsilon_j)} \end{cases} \tag{2}$$

where $\varepsilon_i = n_i^2$ is the dielectric constants, $k_{zi} = \sqrt{k_0^2 n_i^2 - k_x^2}$ is normal component of wave vector in each media, $k_x$ is the tangential component of wave vector which is the same in each layer, $k_0$ is wave vector in vacuum, $\alpha, \beta$ are denominator and numerator of $r_{123}$ and $\sigma = e^2/4\hbar$ is the conductivity of undoped graphene. Without special statement, in the following discussion we use monolayer undoped graphene. Note that $\sigma$ should be set to zero if no graphene is added to the $(i, j)$ boundary. Also note that the Fresnel reflection coefficient $r_{123}$ is not the same as the regular form, because on the boundary of (1,2) there exists graphene layer and $r_{12} \neq -r_{21}$. If graphene between layer (1,2) is removed, $r_{12} = -r_{21}$, $r_{123}$ will return to the regular form. The plus-minus sign in $r_{123}$ refer to TE mode and TM mode respectively.

When incident light is at the resonant angle, PWG mode can be excited. The resonant state is usually analyzed by the zero in the denominator of $R$. However expression of $R$ is complicated and can not give clear physical insight. So following steps described in Ref. 29, we derived the simpler equation by approximating $R$ under conditions $\exp(2ik_{z1}t_1) \ll 1$:

$$R = |r_{01}|^2 \left(1 - \frac{4\Gamma^{\text{int}}\Gamma^{\text{rad}}}{\left[k_x - \text{Re}\left(k_x^0 + \Delta k_x^{\text{rad}}\right)\right]^2 + \left(\Gamma^{\text{int}} + \Gamma^{\text{rad}}\right)^2}\right) \tag{3}$$

Though this equation appears as the same as Ref. 29, we stress that due to addition of graphene the detailed expression of each variable is much more complicated. In Eq. (3) $\text{Re}\left(k_x^0 + \Delta k_x^{\text{rad}}\right)$ is the real part of resonant wave vector of the whole four-layer structure. The $k_x^0$ is resonant wave vector of the three-layer graphene-PWG hybrid structure, where the cladding layers are semi-infinite. $k_x^0$ can be solved by setting denominator of $r_{123}$ to zero, and analytical expression as:

$$\begin{cases} \tan\left(k_{z2}^0 t_2\right) = -i\frac{\Gamma_1 + \Gamma_3}{\Gamma_1\Gamma_3 + 1} \\ \text{TE}: \Gamma_i = \left(k_{zi}^0 + \sigma\omega\mu_0\right)/k_{z2}^0 \\ \text{TM}: \Gamma_i = \frac{k_{z2}^0\varepsilon_i}{k_{zi}^0\varepsilon_2}\left(1 + \frac{\sigma k_{zi}^0}{\omega\varepsilon_0\varepsilon_i}\right) \end{cases} \tag{4}$$

$k_x^0$ can also be solved numerically by FDTD method[30](mode solutions).

$\Delta k_x^{rad} = -r_{01}\exp(2ik_{z1}t_1)\left(\beta/\frac{d\alpha}{dk_x}\right)\Big|_{k_x = k_x^0}$ is caused by finite thickness of cladding layer $t_1$ and the prism layer. And $\Gamma^{\text{int}} = \text{Im}(k_x^0)$ is the internal damping rate, caused by addition of graphene layers to three-layer PWG. The term $\Gamma^{\text{rad}} = \text{Im}(\Delta k_x^{\text{rad}})$ is the radiation damping rate, caused by light escaping from PWG to prism, and mainly attribute to the finite thickness $t_1$. $\Gamma^{\text{rad}}$ is inversely proportional to exponential function of $t_1$, thickness of the first cladding layer. Note that the damping $\Gamma^{\text{rad}}$ does not mean light absorption, on the contrary this part of light escape from PWG, become part of reflected light and reduces light absorption. While $\Gamma^{\text{int}}$ is the damping rate mainly contribute to the light absorption. We can imagine that if $\Gamma^{\text{rad}}$ is too large, light will escape to prism before efficiently absorbed by $\Gamma^{\text{int}}$, while if $\Gamma^{\text{rad}}$ is too small, the PWG mode can not be excited effectively due to large thickness $t_1$. From Eq. (3), we can see that, at resonant state i. e. $k_x = \text{Re}\left(k_x^0 + \Delta k_x^{\text{rad}}\right)$, when $\Gamma^{\text{int}} = \Gamma^{\text{rad}}$ the reflectance become zero, with zero transmittance, the absorbance $A = 1 - R$ will be 1. This can be understood physically as follows, Eq. (3) has a form of Lorentzian-type resonance, $\Gamma^{\text{int}} = \Gamma^{\text{rad}}$ means that the incident light will be absorbed at the same rate as radiated, so all incident light will be absorbed. After the above discussion, we can expect total absorption for specific configuration, and large absorption enhancement can appear with robust structure parameters.

## III. RESULTS AND DISCUSSIONS

In the following analysis, we use TE polarized incident light as illustration and TM mode has similar solutions. In Fig. 2(a), (b), we show figures where total absorption is obtained at wavelength

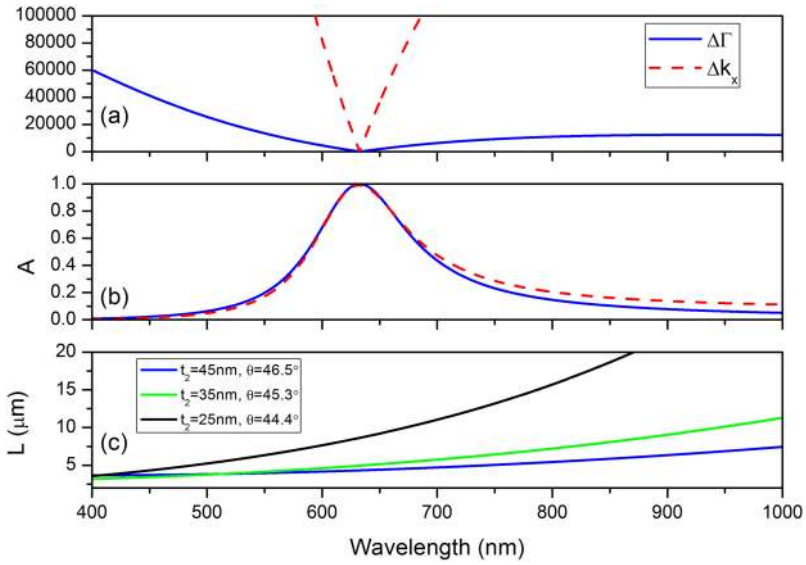


FIG. 2. (a) The wave vector mismatch (blue) and damping rate (red) mismatch. (b) The approximated (blue solid) and precise (red dashed) absorbance. (c) The propagation length with different $t_2$.

633nm. The PWG core is fixed to 45nm thick, first cladding layer $t_1 = 265$nm and light incident angle $\theta = 46.5°$. In Fig. 2(a) we show the wave vector mismatch $\Delta k_x = |k_x - \mathrm{Re}\left(k_x^0 + \Delta k_x^{\mathrm{rad}}\right)|$ (red line) and damping mismatch $\Delta\Gamma = |\Gamma^{\mathrm{int}} - \Gamma^{\mathrm{rad}}|$ (blue line). We can see that at wavelength 633nm, $\Delta k_x = 0$ and $\Delta\Gamma = 0$, the former means that the PWG mode is excited at resonant angle $\theta = 46.5°$ at 633nm, and the latter ensures that total absorption can be obtained. Fig. 2(b) shows the precise absorbance calculated by Eq. (1) (red dashed line) and the approximated absorbance calculated by Eq. (3) (blue solid line). We also examined our precise solution numerically by transfer matrix method (TMM).[31] Though TMM is also derived based on exact analytic equations, it is more like a numerical method. And by comparing TMM result to Eq. (1), we can avoid possible mistakes. As we can see the approximated result fits well with the precise one, which means approximation of Eq. (3) is reasonable. As we expected, at wavelength 633nm, total absorption is achieved. Apart from total absorption at 633nm, strong absorption over 50% has been realized spanning 100nm spectrum from 580nm to 680nm. In Fig. 2(c), we show the propagation length, which is defined by $1/e$ attenuation length of the

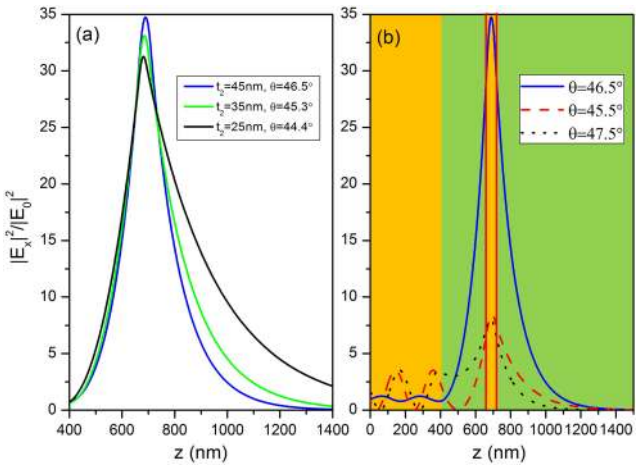


FIG. 3. Normalized tangential electric field intensity distribution at 633nm (a) with different $t_2$, (b) with different $\theta$ and $t_2$ = 45nm.

guided wave intensity, expressed by $L = 1/(2\Gamma^{rad} + 2\Gamma^{int})$. Longer $L$ means that we should fabricate larger device to increase interaction length between graphene and PWG, and shorter $L$ is desired for fabrication convenience. We also show propagation length under different core thicknesses $t_2$ and fix $t_1 = 265$nm. To maintain the resonances at 633nm, different incident angles are used. Generally from Fig. 2(c), for results in Fig. 2(a), (b) the propagation length is in the range of 3 to 8$\mu$m, and at 633nm $L = 4.3\mu$m. As $t_2$ decreases further, the localization of PWG mode decreases, which can be examined by the field distribution shown in Fig. 3(a), as a result propagation length increases. This means that we should design PWG with more localized mode. In Fig. 3 (b), we show the normalized tangential electric field intensity distribution at the resonant state described above (blue line), to understand the absorption enhancement from another perspective. We also show intensity distribution where incident angle is away from resonant, i. e. $\theta = 45.5°$ (red dashed line) and $\theta = 47.5°$ (black dotted line). As we can see, at resonant state the field intensity in the PWG core layer is enhanced by more than 30 times, though graphene has brought considerable internal damping. Stronger field enhancement means that under the same interaction length graphene will absorb more light. And if the incident angle is away from resonance, field enhancement drops quickly in the core layer, lower absorption is obtained then.

In Fig. 4, we show procedures of designing the whole structure in detail. Firstly to excite PWG mode, incident angle should be selected that tangential wave vector in the prism are matched with that of PWG mode, i. e. $k_x = \mathrm{Re}(k_x^0 + \Delta k_x^{rad})$ and $k_x = k_0 n_0 \sin\theta_r$, where $\theta_r$ represents resonant angle in the prism. In Fig. 4(a), we show $\theta_r$ with different thickness of first cladding layer $t_1$ in the wavelength spectrum, $t_1$ = 200, 240, 280nm respectively. These dispersion cures can be solved numerically by solving $k_x = \mathrm{Re}(k_x^0 + \Delta k_x^{rad})$, or precisely by measuring reflectance dips in angular spectrum calculated by TMM method. Here we retrieve $\theta_r$ by the latter method. Note that for each dispersion cure, only at specific wavelength the condition $\Gamma^{int} = \Gamma^{rad}$ is fulfilled, which means total absorption. At other resonant wavelengths of each dispersion cure, though PWG mode can be excited only absorption enhancement can be obtained. This can be seen clearly from Fig. 4(b), where we show $\Gamma^{int}$ (blud line) and $\Gamma^{rad}$ for different $t_1$. $\Gamma^{int}$ is constant for varying $t_1$ for that $k_x^0$ is calculated by three-layer structure without prism, i. e. $t_1$ is semi-infinite. It is clear that each cure of $\Gamma^{rad}$ have only one intersection point with $\Gamma^{int}$, and this point means total absorption. The intersection is at wavelength of 500, 580, 660nm for $t_1$ = 200, 240, 280nm. Finally, we give the absorbance with $t_1$ = 200, 240, 280nm in wavelength spectrum, and the incident angle are chosen to be 48.1°, 47.1°, 46.4° respectively, which are resonant angles searched in Fig. 4(a). As we expected, total absorption occurs at desired wavelength, as shown

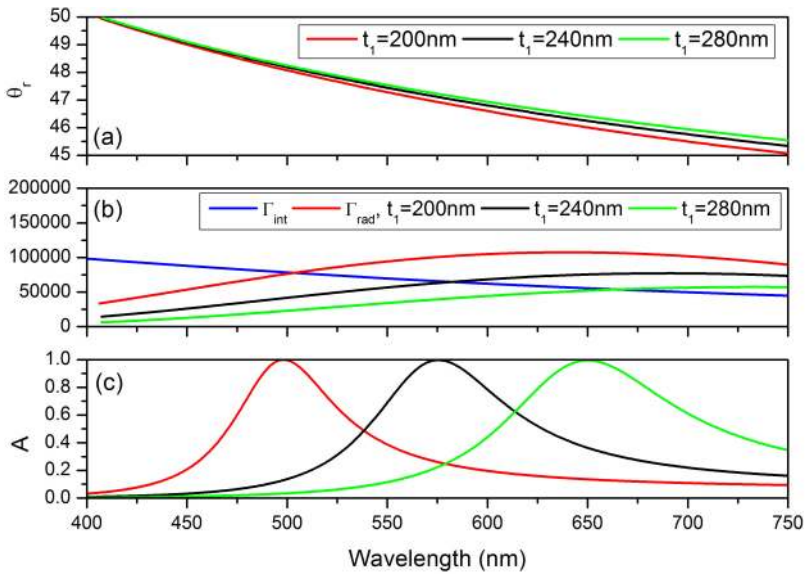


FIG. 4. (a) Resonant angles, (b) internal and radiation damping rate at resonant state, (c) absorbance in wavelength spectrum for different $t_1$.

in Fig. 4(c). From another perspective, if we want to get total absorption at a specific wavelength such as 633nm, we can plot varying $\Gamma^{int}$, $\Gamma^{rad}$ with continuous changed $t_1$, then $t_1$ can be decided by the intersection point, this is also how we decide parameters in Fig. 2. Here we only show results in the visible wavelength range, it is easy to extend our results to larger wavelengths, such as mid-IR to THz ranges, if only we design appropriate waveguide structures and follow procedures discussed above.

As we discussed in the introduction, interband absorption of doped graphene can be suppressed greatly for photon energy below $2E_F$. In our structure, $\Gamma^{int}$ is totally caused by graphene, if total absorption is designed at wavelength near $\lambda = 2\pi\hbar c/(2E_F)$, $\Gamma^{int}$ can be reduced greatly by enhancing $E_F$ though electric doping further. This tunability from total absorption to little absorption can be quite useful for fabrication of optical modulators. As an example, we choose structure parameters in Fig. 2, and total absorption is at 633nm, the corresponding $E_F$ = 0.98eV. In Fig. 5, we show absorbance in wavelength spectrum for $E_F$ = 0.9, 0.98, 1.1eV of doped graphene. During our calculation, we use $\sigma$ of doped graphene expressed by local-RPA model in Ref. 32:

$$\sigma(\omega) = \frac{e^2}{4\hbar}\frac{\mathrm{i}}{(\omega+\mathrm{i}\tau^{-1})}\left[E_{\mathrm{F}}^{T} - \int_0^{\infty} \mathrm{d}E \frac{f_{\mathrm{E}} - f_{-\mathrm{E}}}{1-4E^2/\left[\hbar^2(\omega+\mathrm{i}\tau^{-1})^2\right]}\right] \tag{5}$$

where $E_F$ is the Fermi energy, $E_{\mathrm{F}}^{T} = E_{\mathrm{F}} + 2k_{\mathrm{B}}T\log\left(1+\mathrm{e}^{-E_{\mathrm{F}}/k_{\mathrm{B}}T}\right)$ is for thermal corrections in the doping level, and $f_{\mathrm{E}} = 1/\left[1+\mathrm{e}^{(E-E_{\mathrm{F}})/k_{\mathrm{B}}T}\right]$ is the Fermi-Dirac distribution. Apparently the absorption is greatly reduced from 94% to 5% by enhancing $E_F$ by 0.2eV at 633nm. In realistic devices, $E_F$ of doped graphene can be tuned by adding a relative potential difference $V$. And $|E_F| = \hbar v_F(V\varepsilon_2/4t_2)^{1/2}$, where $v_F = 10^6 m/s$ is the Fermi velocity. For $E_F$ = 1eV, potential of about 4V is obtained.[32] Another method to get high doping levels is using chemically doped graphene first, for example with $E_F$ = 0.9eV, then tune $E_F$ electrically based on this doping level.[16]

Finally, we show result of broadband absorption enhancement at near-IR wavelengths obtained by cascaded multiple PWGs. The cascaded structure is shown in Fig. 1(b), and here we choose 4 PWGs as an example. The corresponding absorbance is shown in Fig. 6(a) calculated by TMM, and parameters are $t_1$ = 240nm, $t_2$ = 45nm, $\theta = 46.25°$. According to Ref. 33, the dispersion cure of 1 PWG will split to 4 cures for 4 PWGs. This is exactly shown in Fig. 6(a), where 4 absorbance peaks appear, and absorbance over 99.9% can be obtained at wavelength 1550nm. Absorbance over 80% can be obtained from 1400nm to 1800nm, over 400nm spectrum range. To compare with, in Fig. 6(b), we show total absorption at 1550nm obtained by single PWG, the parameters are $t_1$ = 750nm, $t_2$ = 100nm, $\theta = 46.15°$. Qualitatively, larger $t_2$ will shift the resonance to larger wavelengths if we fix the incident angle. Or if we fix the resonance wavelength, the incident angle should be larger to excite the PWG mode with lager $t_2$. Apparently absorption enhancement has a narrower bandwidth compared to that in Fig. 6(a). We believe the adding of multilayer graphene broadens the absorption

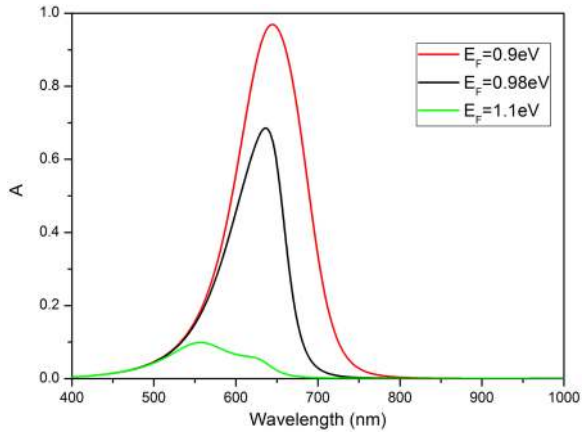


FIG. 5. Absorbance for different $E_F$ = 0.9, 0.98, 1.1eV.

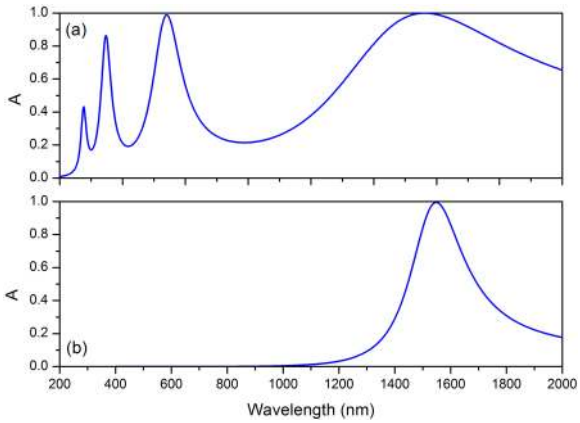


FIG. 6. (a) Absorbance of four cascaded graphene-PWG hybrid structures and (b) single hybrid structure.

enhancement. Qualitatively, when coupled PWG mode is excited, light experiences multiple reflection between different PWG layers, and by interacting with more layers of graphene, the wave attenuated faster, hence fast decay rate broadens the absorption lineshape.

## IV. CONCLUSION

In conclusion, we use ATR configuration to excite PWG mode in a graphene-PWG hybrid structure. After PWG mode is excited, absorption caused by graphene is greatly enhanced, even total absorption can be obtained. We have analyzed principle of total absorption theoretically. The approximated equation deepens our understanding about the origin of total absorption, and also help us design specific hybrid structure. We also show possible application in optical modulators. Finally we have demonstrated a broadband absorption enhancement at near-IR wavelengths by cascading 4 PWGs. We hope our results will be helpful not only in designing optical devices, but also in studying other two-dimensional materials, such as $MOS_2$.

## ACKNOWLEDGMENTS

This work is partially supported by the National Natural Science Foundation of China (Grant No. 61490713, 61575127 and 61505111); Guangdong Natural Science Foundation (Grant No. 2015A030313549); Science and Technology Planning Project of Guangdong Province (Grant No. 2016B050501005).

[1] K. S. Novoselov, A. K. Geim, S. V. Morozov, and A. A. Firsov, Science **306**, 666 (2004).
[2] Q. Bao and K. P. Loh, ACS Nano **6**, 3677 (2012).
[3] F. Bonaccorso, Z. Sun, T. Hasan, and A. C. Ferrari, Nat. Photonics **4**, 611 (2010).
[4] A. N. Grigorenko, M. Polini, and K. S. Novoselov, Nat. Photonics **6**, 749 (2012).
[5] F. J. G. de Abajo, Science **339**, 917 (2013).
[6] M. Liu, X. Yin, E. Ulin-Avila, B. Geng, T. Zentgraf, L. Ju, F. Wang, and X. Zhang, Nature **474**, 64 (2011).
[7] F. Xia, T. Mueller, Y.-M. Lin, A. Valdes-Garcia, and P. Avouris, Nat. Nanotechnol. **4**, 839 (2009).
[8] X. Gan, R. J. Shiue, Y. Gao, I. Meric, T. F. Heinz, K. Shepardand, and D. Englund, Nat. Photonics **7**, 883 (2013).
[9] Q. Bao, H. Zhang, B. Wang, Z. Ni, C. H. Y. Xuan Lim, Y. Wang, D. Y. Tang, and K. P. Loh, Nat. Photonics **5**, 411 (2011).
[10] Y. Lu *et al.*, J. Opt. Soc. Am. B **33**, 1842 (2016).
[11] A. Y. Nikitin, F. Guinea, F. J. Garcia-Vidal, and L. Martin-Moreno, Phys. Rev. B **85**, 081405 (2012).
[12] R. Alaee, M. Farhat, C. Rockstuhl, and F. Lederer, Opt. Express **20**, 28017 (2012).
[13] Z. Fang, Y. Wang, A. E. Schlather, Z. Liu, P. M. Ajayan, F. J. G. de Abajo, and N. J. Halas, Nano Lett. **14**, 299 (2013).
[14] S. Thongrattanasiri, F. H. Koppens, and F. J. G. de Abajo, Phys. Rev. Lett. **108**, 047401 (2012).
[15] M. A. K. Othman, C. Guclu, and F. Capolino, Opt. Express **21**, 7614 (2013).
[16] F. J. G. de Abajo, Acs Photonics **1**, 135 (2014).
[17] A. Ferreira, N. M. R. Peres, R. M. Ribeiro, and T. Stauber, Phys. Rev. B **85**, 115438 (2012).
[18] M. Furchi, A. Urich, A. Pospischil, G. Lilley, K. Unterrainer, H. Detz, and T. Mueller, Nano Lett. **12**, 2773 (2012).
[19] J. T. Liu, N. H. Liu, J. Li, X. J. Li, and J. H. Huang, Appl. Phys. Lett. **101**, 052104 (2012).
[20] J. R. Piper and S. Fan, ACS Photonics **1**, 347 (2014).

[21] Y. Cai, J. Zhu, and Q. H. Liu, Appl. Phys. Lett. **106**, 043105 (2015).
[22] Y. Wu, J. Niu, M. Danesh, J. Liu, Y. Chen, L. Ke, C. Qiu, and H. Yang, Appl. Phys. Lett. **109**, 041106 (2016).
[23] G. Pirruccio, L. Martin Moreno, G. Lozano, and J. Gomes Rivas, ACS nano **7**, 4810 (2013).
[24] L. Zhu, F. Liu, H. Lin, J. Hu, Z. Yu, X. Wang, and S. Fan, Light: Sci. Appl. **5**, e16052 (2016).
[25] E. F. C. Driessen and M. J. A. de Dood, Appl. Phys. Lett. **94**, 171109 (2009).
[26] W. Zhao, K. Shi, and Z. Lu, Opt. Lett. **38**, 4342 (2013).
[27] Q. Ye, J. Wang, Z. Liu, Z. Deng, X. Kong, F. Xing, X. Chen, W. Zhou, C. Zhang, and J. Tian, Appl. Phys. Lett. **102**, 021912 (2013).
[28] C. R. Dean, A. F. Young, I. Meric, C. Lee, L. Wang, S. Sorgenfrei, and J. Hone, Nat. nanotechnology **5**, 722 (2010).
[29] T. Okamoto, M. Yamamoto, and I. Yamaguchi, J. Opt. Soc. Am. A **17**, 1880 (2000).
[30] K. J. A. Ooi, L. K. Ang, and D. T. H. Tan, Appl. Phys. Lett. **105**, 111110 (2014).
[31] T. Zhan, X. Shi, Y. Dai, X. Liu, and J. Zi, J. Phys.: Condens. Matter **25**, 215301 (2013).
[32] R. Yu, V. Pruneri, and F. J. G. de Abajo, ACS Photonics **2**, 550 (2015).
[33] P. Yeh, A. Yariv, and C. S. Hong, J. Opt. Soc. Am. **67**, 423 (1977).